EarthArXiv Cover Page

Why is it critical to revisit significance and consequences of salt precipitation during CO_2 injection?

Mohammad Nooraiepour [1,*], Mohammad Masoudi[1], Helge Hellevang[1], Karol Dąbrowski[2], Szymon Kuczyński[2], Michał Zając[2], Stanisław Nagy[2] and Rafał Smulski[2]

[1] Department of Geosciences, University of Oslo, P.O. Box 1047 Blindern, 0316 Oslo, Norway
[2] AGH University of Science and Technology, Mickiewicza 30 Av, 30-059 Kraków, Poland
* Correspondence: mohammad.nooraiepour@geo.uio.no

Introduction

The global concern about the consequences of climate change and global warming has led to a search for environmental, technological, and economical solutions to mitigate adverse effects caused by human-made emissions of greenhouse gases atmospheric, particularly carbon dioxide (CO_2). Carbon capture and storage (CCS) is one of the promising accessible near-term solutions. Among the different candidates for subsurface CO_2 storage, deep saline aquifers are considered the best option regarding storage capacity and proximity to emission sources.

Injection of large volumes (ideally, million tons scale) of undersaturated supercritical CO_2 (with respect to water) into the geological formations causes evaporation of formation water, increase in the concentration of the dissolved salts in brine pore fluid, and eventually under the thermodynamic conditions of a given storage reservoir, solute concentration will reach the solubility limit and precipitate out of the aqueous phase leading to precipitation of salt crystals inside the porous media (Nooraiepour et al., 2018a,b). CO_2-induced salt precipitation can substantially threaten sequestration in saline aquifers (Masoudi et al., 2021). It reduces the reservoir permeability around wellbore, induces pressure buildup, and causes a decline in injectivity. Inducing excess pressure buildup may cause caprock fracturing near injection wells. Moreover, salt crystals' precipitation harms the economy because it reduces injection efficiency, causes operational delays, and requires costly remediation campaigns and injection cessation.

Most available experimental, numerical and theoretical works have focused on predicting the precipitated salt's location and amount. However, less attention is given to the precipitation physics, growth dynamics, and behavior of the fluid-solid interface near the evaporation/precipitation front (Masoudi, 2021; Nooraiepour et al., 2018a,b). One notable common shortcoming is neglecting access to in-situ brine sources within the saline aquifers, which can dramatically reshape the dynamics and dimensionality of mineral/crystal growth in porous reservoir rocks owing to the availability and continuity of solute. Here, we report a series of experiments (droplets, precipitation/growth on various substrates, lab-on-chip, glass-microchips, HPHT geomaterial microfluidics, and synthetic porous structures with glass beads) to provide new insights, beyond the current state of understanding, into the dynamics of brine evaporation and salt precipitation/growth and to challenge the current understanding that might not be entirely representative of thermodynamic conditions observed in the field.

Materials and Methods

The precipitation and growth experiments were conducted using a variety of salt crystals present in formation waters of candidate saline aquifers and seawater. We prepared stock solutions of crystalline solids (ACS reagent, ≥ 99.8%) of anhydrous and hydrous salts such as sodium chloride (*NaCl*), sodium sulfate (Na_2SO_4), potassium chloride (*KCl*), sodium bicarbonate ($NaHCO_3$), potassium bromide (*KBr*), magnesium chloride ($MgCl_2.6H_2O$), and calcium chloride ($CaCl_2.2H_2O$). The well-defined weight of crystalline salts was dissolved in the deionized water (DI-water) [Milli-Q water] to prepare stock solutions of varying concentrations (salinity). We used the PHREEQC v3 for aqueous geochemical calculations to compute solute supersaturation before the experiments (Nooraiepour et al., 2021a). Moreover, artificial seawater was also prepared, according to the ASTM D1141-98. Additionally, we sampled approximately 1 liter of Oslo Fjord seawater and filtered fluid through a 0.45 µm Millipore© filter. In the Oslo Fjord, the seawater is only slightly affected by the inflow of freshwater mixing but shows a close chemical composition to average North Sea seawater (Nooraiepour et al., 2022).

The microfluidic experiments were conducted at 1-10 MPa injection pressure, 20-60°C temperature, and 0.5-25 cm^3 CO_2/min flow rates. The flow of CO_2, therefore, was investigated for gaseous, supercritical, and liquid phase states. Comparing several flow rates provided a measure to evaluate the impact of viscous forces against the capillary forces and examine the possibility of mitigating or minimizing salt precipitation events. In microfluidic studies, geomaterial (homogenous and heterogeneous sandstone, carbonate, and shale rock samples) and glass (soda–lime and borosilicate) substrates were used. Further details of the laboratory apparatus are given in Fazeli et al. (2020) and Moghadam et al. (2019). Droplet tests, lab-on-chip growth dynamics, and precipitation geometry in synthetic porous media (out of glass beads of different sizes) were also performed at different salinities, solute types, and evaporation rates

(temperatures). A CO_2 bottle (grade 5.2, scientific carbon dioxide) was used. Nitrogen and pressurized purified air were also used as carrier gases to evaporate brine and salt precipitation.

Pore-scale precipitation and growth of various salt crystals inside the porous media and on top of solid substrates were monitored and visualized in real-time under bright field imaging using different techniques fit for a given experiment, namely, (a) advanced polarized light microscopy (20X, Nikon Instruments Inc.), (b) Nikon SMZ stereo microscope, (c) high-resolution Dino-Lite digital microscope, and (d) a full-frame Nikon Z 7II mirrorless camera. For post-experiment analysis of three-dimensional geometry and porous structure of salt bodies Scanning electron microscopy (SEM), backscattered (BSE) and secondary electrons (SE) imaging, was used. In addition, energy-dispersive x-ray spectroscopy (EDS) was used for chemical analyses and element mapping (spatial resolution of 1 µm).

Results and Discussion

The microfluidic laboratory experiments showed that the conditions (reservoir pressure-temperature) and phase states (gaseous, supercritical, and liquid CO_2) control the probabilistic dynamics of precipitation and growth of salt crystals in saline aquifers. The results indicate influencing magnitude, distribution, and growth patterns. In Figure 1a, the water solubility in CO_2 (H_2O mol %) is calculated based on the statistical associating fluid theory (SAFT), determining the capability of injected carbon dioxide as the carrier gas for drying out the porous media. SAFT is a semiempirical equation of state for modeling thermodynamic properties and accurately handling multicomponent phase equilibria at low and high pressures for fluid mixtures. The cross-plot of Figure 1b presents the maximum water flux into the CO_2 versus the total salt coverage for each experiment. It presents the percentage of salt surface coverage during the microfluidic experiment at different thermodynamic conditions. Within the pressure-temperature interval of this study, the increase in injection pressure results in a decrease in total salt precipitation. The maximum water influx (H_2O mol %) during the experiments is derived by multiplying the volume of injected CO_2 by water solubility in CO_2 at the pressure-temperature condition of a given experiment, as given in Figure 1a. It demonstrates with a relatively strong correlation (exponential relationship, $R^2 \approx 0.9$) that the higher the maximum water flux, the higher the salt coverage. The data points for the liquid and $scCO_2$ phases are located at the bottom left of the plot. In contrast, the tests with gaseous CO_2 are extended to the top right of the plot, where higher water flux is calculated, and extensive salt accumulations are observed. In addition to the impact of maximum water flux, another observation was noted for the liquid and $scCO_2$ phases. When the dense phases (liquid and $scCO_2$) were injected, more brine was flushed out of the porous geometry, and lower residual saturation was established because of the higher imposed viscous forces. Consequently, it caused lower residual brine and limited precipitation of micrometer-sized salt crystals.

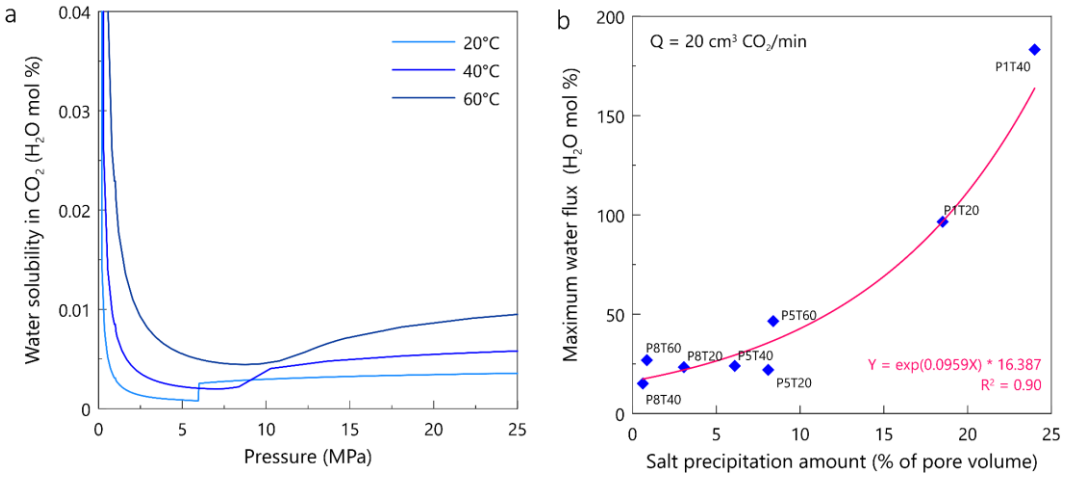

Figure 1 *(a) Water solubility in CO_2 (H_2O mol %) as a function of pressure (MPa) and temperature (°C), calculated via the statistical associating fluid theory (SAFT). (b) Effect of thermodynamic conditions and CO_2 phase states on salt surface coverage during microfluidic experiments, where maximum water flux is plotted versus salt surface coverage of total porosity. P= pressure, T= temperature, and Q= flow rate.*

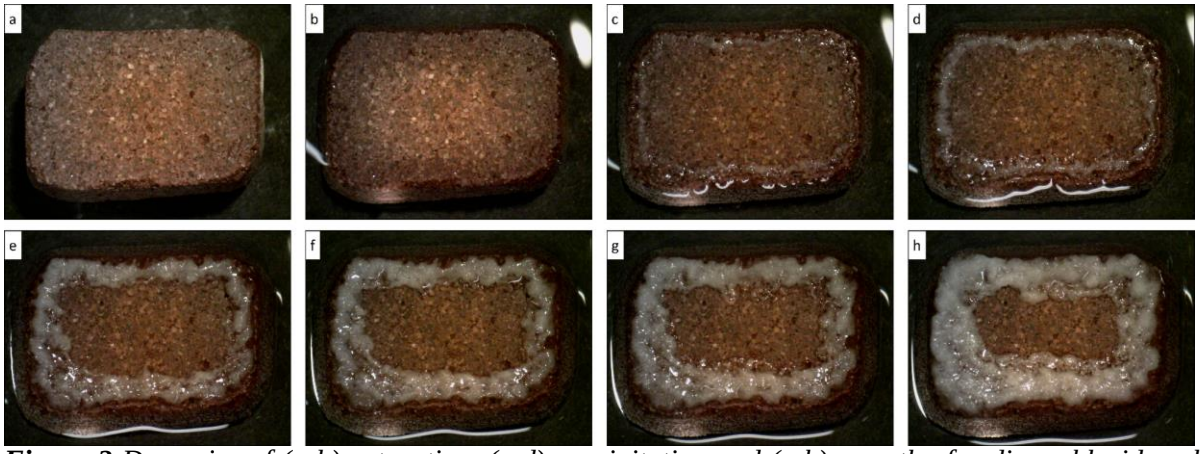

Figure 2 *Dynamics of (a-b) saturation, (c-d) precipitation and (e-h) growth of sodium chloride salt crystal on the surface of a porous reservoir rock. Imbibing brine toward the salt bodies and transporting water films carrying solute toward the evaporation sites are evident in the bottom row.*

The results of performed experiments show that: (i) salt crystals occurs as at least two distinct forms (single isolated crystals and micrometer-sized accumulations), (ii) salt precipitation and growth is not limited to residual brine inside the porous medium, (iii) crystals growing within/into the CO_2 stream has the highest potential for blocking flow pathways and deteriorating permeability, (iv) precipitation and growth is a dynamic and time-evolving phenomenon supported via self-enhancing nature, (vi) the capillary suction transports continuous water films towards the evaporation front, (vii) thermodynamic control is significant factor, (viii) the interplay between CO_2 phase states, critical velocity, and injection rate need to be considered for evaluating fate of subsurface flow and transport , (ix) the mutual impact of viscous and capillary forces affect the growth dynamics, and finally (x) the affinity of salt crystals (different crystals to a different degree) for water will result in bigger salt patches inside the saline aquifer reservoirs. The observed characteristics called for a further in-depth investigation because, in the context of subsurface CO_2 storage, we need to redefine how we see injectivity impairment due to salt precipitation.

Figure 2 shows how the reservoir rock in saline aquifers that have access to the infinite source of solute (dissolved salts in brine formation water) may provide continuous and conductive water film flow across the water-wet substrate surfaces towards the evaporation front. The continuous and plentiful brine support cannot be precisely reproduced in most flow experiments and, therefore, cannot capture the entire dimensionality of potential issues due to injectivity impairment.

It is critical (and an open question) to identify the entire length scale over which capillary-driven backflow of brine and suction towards the evaporation front occurs and determine the total salt mass transported to the precipitation front. We hypothesized previously that the porous structure of salt bodies imposes capillary forces. The preliminary results of SEM structural identifications suggest that there might be both porous (micro to nano) and non-porous (nano to none) CO_2-induced salt accumulations inside the porous media. Quantifying these porous structures lays the foundation for estimating the potential for imposing capillary forces by the growing body of salts inside reservoir rocks.

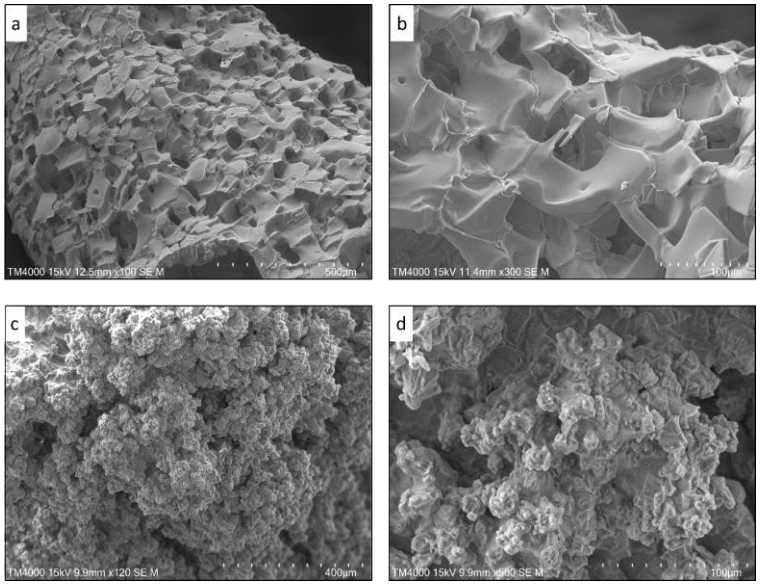

Figure 3 *Scanning electron microscopy of porous and non-porous CO_2-induced salt precipitation within porous media.*

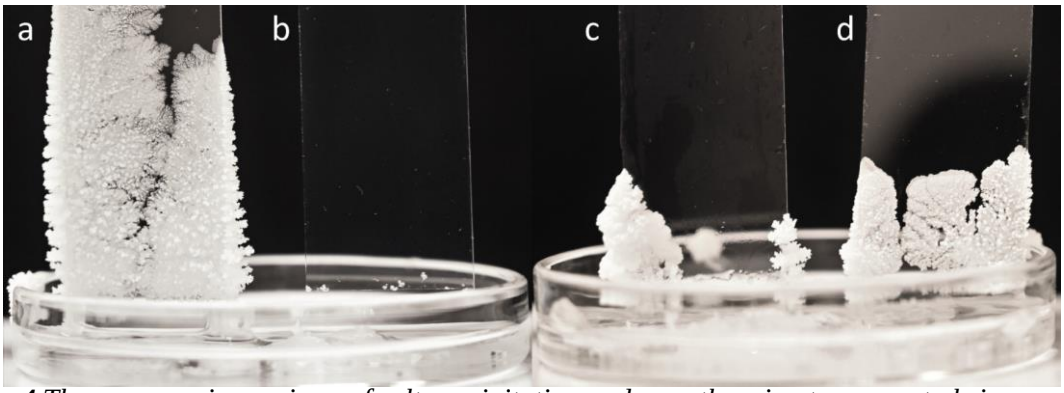

Figure 4 *Three successive regimes of salt precipitation and growth owing to access to brine sources.*

Figure 4 documents three regimes and precipitation waves delineating dynamics of salting-out owing to solute transport towards the evaporation sites and supporting nucleation and growth on secondary precipitates in competition to the primary foreign substrate (Masoudi et al., 2022; Nooraiepour et al., 2021b).

Conclusions

The research outcome highlights the interplay of complex processes (some of which are not yet fully characterized) crucial in investigating salt precipitation induced by million-tons-scale CO_2 injection. For precise predictions and reservoir-scale numerical modeling, the underlying physics, governing factors, and a physically representative scale-up workflow must be incorporated into the continuum-scale reservoir simulator. Furthermore, delineating the porous structure of salt accumulations, all three waves of precipitation, and the significance of access to infinite solutes in saline aquifers requires further scrutiny.

Acknowledgements

The authors would like to acknowledge the funding support by the "solid and salt precipitation kinetics during CO_2 injection into reservoir (SaltPreCO2)" project (Norway Grants, Norwegian Financial Mechanism 2014-2021 under GREIG Programme, UMO-2019/34/H/ST10/00564).

References

Fazeli, H., Nooraiepour, M., and Hellevang, H. [2020]. Microfluidic study of fracture dissolution in carbonate-rich caprocks subjected to CO_2-charged brine. ACS I&EC Research, 59(1).

Hellevang, H., Wolff-Boenisch, D., and Nooraiepour, M. [2019]. Kinetic control on the distribution of secondary precipitates during CO_2-basalt interactions. E3S Web of Conferences, 98.

Masoudi, M., Fazeli, H., Miri, R., and Hellevang, H. [2021]. Pore scale modeling and evaluation of clogging behavior of salt crystal aggregates in CO_2-rich phase during carbon storage. International Journal of Greenhouse Gas Control, 111, 103475.

Masoudi, M. [2021]. Near wellbore processes during carbon capture, utilization, and storage (CCUS): An integrated modeling approach. Doctoral thesis, University of Oslo, pp. 206.

Masoudi, M.; Nooraiepour, M.; Hellevang, H. [2022]. The effect of preferential nucleation sites on the distribution of secondary mineral precipitates. Proceedings of the 83rd EAGE Annual Conference & Exhibition, June 2022, Madrid, Spain.

Moghadam, J.N., Nooraiepour, M., Hellevang, H., Mondol, N. H., and Aagaard, P. [2019]. Relative permeability and residual gaseous CO_2 saturation in the Jurassic Brentskardhaugen Bed sandstones, western central Spitsbergen, Svalbard. Norwegian Journal of Geology, 99(2), 1–12.

Nooraiepour, M., Fazeli, H., Miri, R., and Hellevang, H. [2018a]. Effect of CO_2 phase states and flow rate on salt precipitation in shale caprocks - A microfluidic study. ACS ES&T, 52(10), 6050–6060.

Nooraiepour, M., Fazeli, H., Miri, R., and Hellevang, H. [2018b]. Salt precipitation during injection of CO_2 into saline aquifers: Lab-on-chip experiments on glass and geomaterial microfluidic specimens. 14th Greenhouse Gas Control Technologies Conference (GHGT-14), October 2018, Melbourne, Australia.

Nooraiepour, M., Masoudi, M., Shokri, N., and Hellevang, H. [2021a]. Probabilistic nucleation and crystal growth in porous medium: New insights from calcium carbonate precipitation on primary and secondary substrates. ACS Omega, 6(42), 28072–28083.

Nooraiepour, M., Masoudi, M., and Hellevang, H. [2021b]. Probabilistic nucleation governs time, amount, and location of mineral precipitation and geometry evolution in the porous medium. Scientific Reports 11, 16397.

Nooraiepour, M., Masoudi, M., Shokri, N., and Hellevang, H. [2022]. Precipitation-induced geometry evolution in porous media: Numerical and experimental insights based on new model on probabilistic nucleation and mineral growth. Proceedings of the 16th Greenhouse Gas Control Technologies Conference (GHGT-16), October 2022, Lyon, France.